Conservative Implementation of LES-CMC for Turbulent Jet Flames

P. Siwaborworn and A. Kronenburg

Abstract The objective of the present work is to validate a large eddy simulation (LES) approach that has been coupled with a conditional moment closure (CMC) method for the computation of turbulent diffusion flames. Contrary to earlier work, we use a conservative implementation of CMC that ensures mass conservation of the fluxes across the computational cell faces. This is equivalent to a weighting of the fluxes by their probabilities at the cell faces, and it is thought that this weighting leads to a more dynamic response of the conditionally averaged moments to temporal changes induced by the large scale turbulent motion. The first application to the Sandia Flame Series D-F allows for the validation of the method, but further studies with different flame geometries and more pronounced large scale instationary effects will be needed for the demonstration of the benefits of conservative CMC when compared to the conventional (non-conservative) implementation.

1 Introduction

The Large eddy simulation (LES) approach is considered to be the most promising approach for the computation of turbulent flows in applications of engineering interest. LES solves large scales of turbulent flows up to grid sizes using spatial filtering and models subgrid scales using Smagorinsky model. CMC is applied for a turbulent combustion modelling using mixture fraction as a conditional variable. A non-conservative LES-CMC has provided predictions of major and minor species for different flames in a last decade. However, inaccurate predictions occur in CMC cells which have large temporal variations of the mixture fraction field. A lack of FDF-weighting (filtered density function) ratios in a convective term of the non-conservative CMC is believed to be the main reason for inaccurate predictions.

P. Siwaborworn (✉) · A. Kronenburg
Institut für Technische Verbrennung, University of Stuttgart, Stuttgart, Germany
e-mail: p.siwaborworn@itv.uni-stuttgart.de; kronenburg@itv.uni-stuttgart.de

In contrast to non-conservative LES-CMC, the present conservative formulation is inherently mass conserving. It considers FDF-weighting ratios in convective term so that improved predictions of local conditional scalars can be obtained.

In this work, investigations of turbulent jet flames (Sandia Flame D, E and F) are performed by the conservative LES-CMC approach. Flame D is used as the first test case to validate the numerical results by comparison with well-established experimental data. Subsequently, Flames E and F are investigated for extinction and reignition phenomena. Computational results of the present work from using HLRS resources are given first. Subsequently, the computational resources which have been used to simulate Sandia Flames series will be addressed.

2 Results of the Present Work

In this section, the computational setups are described, followed by the summaries of parametric CMC studies in Sect. 2.2. Section 2.3 presents the simulation results for Sandia Flame D, which is carried out as the first test case in order to validate the LES-CMC simulation models as a reference. Predictions of Flame D are also chosen as representatives in this paper, since the simulation results of Flames E and F follow the same tendency as predictions of in Flame D. This section closes with the discussion and conclusions about the performance of various CMC model parameters in Sect. 2.4.

2.1 Computational Setup

Computational grid was generated with dimensions of $80D$ in z-direction and $8D$ in x- and y-directions at the flame base increasing to $60D$ at the outlet of the domain. Fine grid simulations of Sandia Flame series, having $112 \times 112 \times 320$ cell grids for LES and $8 \times 8 \times 80$ cell grids for CMC (reference case), have been carried out with HLRS resources. The regions above the jet and pilot are captured by 28 and 40 LES cells (for a dimension), respectively. Due to grid independence studies by Navarro et al. [1], these computational cells satisfy a condition that the largest fraction of energy spectrum is resolved after the initial break-up of the jet. The CMC grid has 100 nodes in mixture fraction space which has refinement at $\eta = 0$ and 1.

2.2 Parametric Studies

The results of the LES-CMC modelling are presented in three main parts. Parametric studies of flow and mixing field, parametric studies of combustion model and parametric study of CMC grid resolution are investigated in order to study the effects

of each parameter on simulation results. Details of these studies for each parameter
are given in the following sections.

2.2.1 Parametric Studies of Flow and Mixing Field

The parametric studies of flow and mixing field are the inflow velocity variances in
turbulent inflow generator, the Schmidt number, Sc, the turbulent Schmidt number,
Sc_t, and constant value, C_ξ, which is used in modelling of the variance of mixture
fraction ($\widetilde{\xi''^2_{sgs}} = C_\xi \Delta^2 \left(\frac{\partial \tilde{\xi}}{\partial x_j} \frac{\partial \tilde{\xi}}{\partial x_j} \right)$). Besides C_ξ, all of them are fluid properties
which actually are not allowed to be changed. However, the velocity variance levels
are adjusted to yield suitable values for the inflow generator which creates the
oscillation of the velocity field in this work. The Schmidt number and the turbulent
Schmidt number, which are the ratios of momentum transfer rate to mass transfer
rate for resolved and unresolved scales, are varied to test a sensitivity of the flow
and mixing field. Sandia Flame D is used as a reference case and thus simulation
results from these optimal values are reported in Sect. 2.3.

2.2.2 Parametric Studies of Combustion Model

The evaluation of the LES-CMC combustion model is in the focus of the present
research project. The parametric studies concerning the combustion model carried
out here comprise the evaluation of the CMC formulation, the approximation of
the CMC convective fluxes and the model for the conditionally filtered turbulent
diffusivity.

- CMC Formulations

   The difference of the two CMC formulations (the non-conservative form in
   Eq. 1 and the conservative form in Eq. 2) is the inclusion of the FDF information
   into the transport equation, in particular into the convective term (the second term
   on the LHS) of the conservative CMC formulation.

$$\frac{\partial Q_\alpha}{\partial t} + \widetilde{u}_{j,\eta} \frac{\partial Q_\alpha}{\partial x_j} - \frac{1}{\gamma} \frac{\partial}{\partial x_j} \left(\gamma D_\eta \frac{\partial Q_\alpha}{\partial x_j} \right) = \tilde{w}_{\alpha,\eta} + \widetilde{N}_\eta \frac{\partial^2 Q_\alpha}{\partial \eta^2}, \qquad (1)$$

$$\gamma \frac{\partial Q_\alpha}{\partial t} + \frac{\partial}{\partial x_j} (\gamma \widetilde{u}_{j,\eta} Q_\alpha - \gamma D_\eta \frac{\partial Q_\alpha}{\partial x_j}) = \gamma \tilde{w}_{\alpha,\eta} + \gamma \widetilde{N}_\eta \frac{\partial^2 Q_\alpha}{\partial \eta^2} + Q_\alpha \frac{\partial}{\partial x_j} (\gamma \widetilde{u}_{j,\eta}), \qquad (2)$$

where γ denotes $\bar{\rho} \widetilde{P}(\eta)$ and $\widetilde{P}(\eta)$ is the Favre filtered probability density
function (FDF). $Q_\alpha = \widetilde{Y_\alpha \mid \eta}$ is the conditionally filtered mass fraction. $\widetilde{u}_\eta$ is
the conditionally filtered velocity, $\tilde{w}_\eta$ is the conditionally filtered reaction source
term and $\widetilde{N}_\eta$ is the conditionally filtered scalar dissipation rate. Term $D_\eta \frac{\partial Q_\alpha}{\partial x_j}$ is

the modelled -by using of a gradient diffusion approximation- of the subgrid-scale conditional scalar flux. Based on finite volume method, both conditional species transport equations can be applied to each control volume (CV) of the computational domain. It is believed that including the FDF information in convection will make the CMC conservative form more precise than the traditional one [2]. Therefore, the study of two different formulations of the combustion model is performed in this work to reveal the results of the assumption.

- Flux Approximations

  Since each CMC cell comprises of a number of LES cells, two methods can be applied to approximate the convective flux between CMC cells. The first method calculates convective flux over the CMC cell face from the convective fluxes of the LES cells adjacent to the CMC cell face. The second method computes convective flux from the values at the CMC cell centre, which takes into account the values of all LES cells within the CMC cell. The convective flux from the first method is shown as the summation of the small arrows in Fig. 1, while the convective flux from the second method is shown as the big arrow in the same figure.

- Conditionally Filtered Turbulent Diffusivity Models

  There are three methods to model the conditionally filtered turbulent diffusivity, D_η. However, all of them are based on the Smagorinsky model for the subgrid-scale kinematic viscosity, v_t and the relation of unconditionally filtered turbulent diffusivity, $D_t = v_t/Sc_t$. In the first method, D_η is calculated based entirely on CMC cell (named $D_{\eta,1}$). Therefore, v_t in this method is calculated based on CMC grid resolution. In the second method, $D_{\eta,2}$ is calculated based on D_t from every LES cell which locate inside that CMC cell. The ensemble averaging over a CMC cell can be computed by weighting with FDF. In the third method $D_{\eta,3}$, the ratio of the size of CMC cell to LES cell is included into the second method in order to adjust the length scale during modelling D_η value. This additional value is hoped to predict more accurately since the D_η model should be based on the filter width of CMC instead of on the filter width of LES.

2.2.3   Parametric Study of the CMC Grid Resolution

Another main parametric study for all Sandia Flame series is the CMC grid resolution. For a simple and stable flame, this parameter might not reveal any effect. However, it is believed that a high number of CMC cells may capture the extinction and reignition phenomena due to the turbulence-chemistry interactions in Flames E and F. Thus, three CMC grid resolutions are performed in this study topic. These are $4 \times 4 \times 80$, $8 \times 8 \times 80$ and $16 \times 16 \times 80$ CMC cells for the same LES resolution.

To summarize, all parametric studies are shown in Table 1 and they were varied for Flame D. The values resulting in the best agreement between simulation and experiments of parametric studies of flow and mixing field of Flame D were chosen for further simulations of Flames E and F.

Fig. 1 A schematic of the two approximations of the CMC convective flux
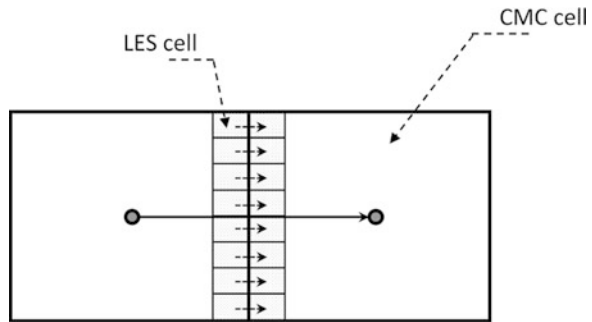
2.3 Results of Sandia Flame D

Results of Sandia Flame D are composed of three principal parts. Firstly, results of the parametric studies of flow and mixing field are reported. Subsequently, results of the parametric studies of combustion model are shown and discussed. Finally, results of the parametric study of CMC grid resolution are given and discussed.

2.3.1 Parametric Studies of the Flow and Mixing Field

Using a reference case of parametric studies in combustion model (CMC-1, flux-1 and $D_{\eta,2}$) and CMC grid resolution of $8 \times 8 \times 80$, the best results of parametric studies in flow and mixing fields are variance-2, Sc_2, $Sc_{t,1}$ and $C_{\xi,1}$. The meaning of each parameter can be found in Table 1. Overviews of best results in flow and mixing filed which use these optimum values can be observed in Figs. 2 and 3.

Figure 2 shows a snapshot of the instantaneous temperature field along a 2D plane through the burner centerline for the whole computational domain (left) and focused on the upstream region (right). The black lines indentify the isoline of stoichiometric mixture fraction. It can be observed from a temperature profile (Fig. 2 (right)) that there is a high level of turbulence which comes from the digital turbulent inflow generator at the inlet. Moreover, the local extinction, which would be characterized by discontinuous red color of the temperature along the isoline of stoichiometric mixture fraction, hardly occurs in Flame D, in accordance with the experimental findings.

Radial profiles of mean and RMS axial velocity and mixture fraction at three downstream locations are shown in Fig. 3. Both mean and RMS of axial velocity and mixture fraction agree properly with the experiments [3,4], since the effects of initial inflow from inflow generator are previously checked and adjusted. Moreover, it can be seen form Fig. 3 that the jet spreading is captured well. Small overpredictions of the mean mixture fraction in the range of $1.2 < r/D < 2$ at position $z/D = 3$ may come from the influences of lateral boundary conditions. Small overpredictions

Table 1 Summary of parameters studies

Quantity	Name	Values or methods
Variances of inflow generator	variance-1	$u'u'$, $v'v'$ and $w'w'$ [3]
	variance-2	$\frac{2}{3}u'u'$, $\frac{2}{3}v'v'$ and $\frac{2}{3}w'w'$
Schmidt number	Sc_1	0.4
	Sc_2	0.7
	Sc_3	1.0
Turbulent Schmidt number	$Sc_{t,1}$	0.4
	$Sc_{t,2}$	0.7
Variance of mixture fraction	$C_{\xi,1}$	0.2
	$C_{\xi,2}$	0.3
CMC formulation	CMC-1	Conservative CMC
	CMC-2	Non-conservative CMC
Convective flux	flux-1	Computing fluxes based on LES cells at CMC faces
	flux-2	Computing fluxes based on CMC cell centers
Conditionally filtered turbulent diffusivity	$D_{\eta,1}$	Modelling D_η based on CMC cells
	$D_{\eta,2}$	Modelling D_η based on LES cells
	$D_{\eta,3}$	Modelling D_η with adjusting the length scale
Number of CMC cells	$4 \times 4 \times 80$	4 CMC cells in X- and Y-directions with 80 CMC cells in Z-direction
	$8 \times 8 \times 80$	8 CMC cells in X- and Y-directions with 80 CMC cells in Z-direction
	$16 \times 16 \times 80$	16 CMC cells in X- and Y-directions with 80 CMC cells in Z-direction

of the mean axial velocity and mixture fraction around $1 < r/D < 2$ at position $z/D = 15$ may require more simulation time for more precision. However, the current predictions provide a good basis for the parametric studies of combustion model.
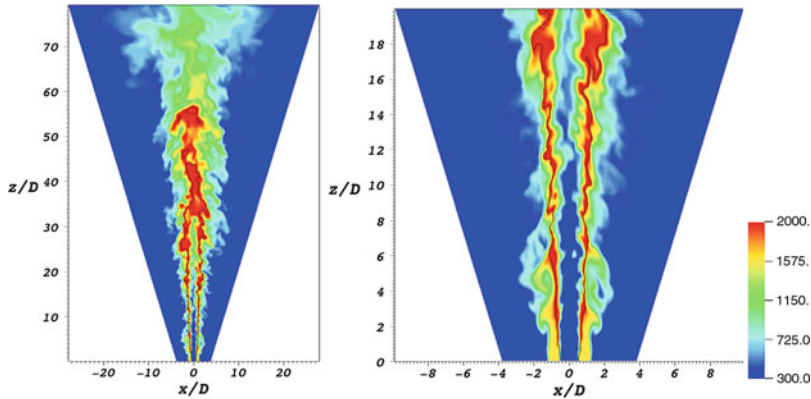
Fig. 2 Snapshots of the temperature field in total computational domain (*left*) and in the upstream region (*right*) for Sandia Flame D. The iso-contour of stoichiometric mixture fraction is presented by the *black lines*

2.3.2   Parametric Studies of the Combustion Model

As shown in Table 2, five case studies are performed to show the effects of each case in CMC model. All cases are based on the optimal conditions from parametric studies of flow and mixing field (variance-2, Sc_2, $Sc_{t,1}$ and $C_{\xi,1}$) and use $8 \times 8 \times 80$ for the number of CMC cells. A reference case (case-1) includes the models CMC-1, flux-1 and $D_{\eta,2}$, while other cases have at least one varied parameter compared with the reference case.

Preliminary Studies

Preliminary studies of parametric studies of combustion model are required to choose the cases which may predict the simulation results different from the reference case (case-1 from Table 2). These case studies will be further examined for the simulation results in next sections. In the first step, a representative direction has to be defined. Having the highest convective value among three directions, the convective flux in z−direction is chosen as a representative. Note that a consideration of FDF profile is required, since it is applied to transfer the values from a mixture fraction space to a physical space. The low value of FDF means only a small influence of any property can appear in the physical space.

Subsequently, the convective fluxes in z−direction are shown in radial and axial distributions. The instantaneous predictions of CH_4 fluxes in Fig. 4 show that the radial distribution exhibits larger differences of the convective fluxes between each case than the axial distribution. Thus, the radial distribution is applied for investigations of convective flux comparisons for the other species. It should be reminded that a consideration of FDF is necessary as previously discussed.
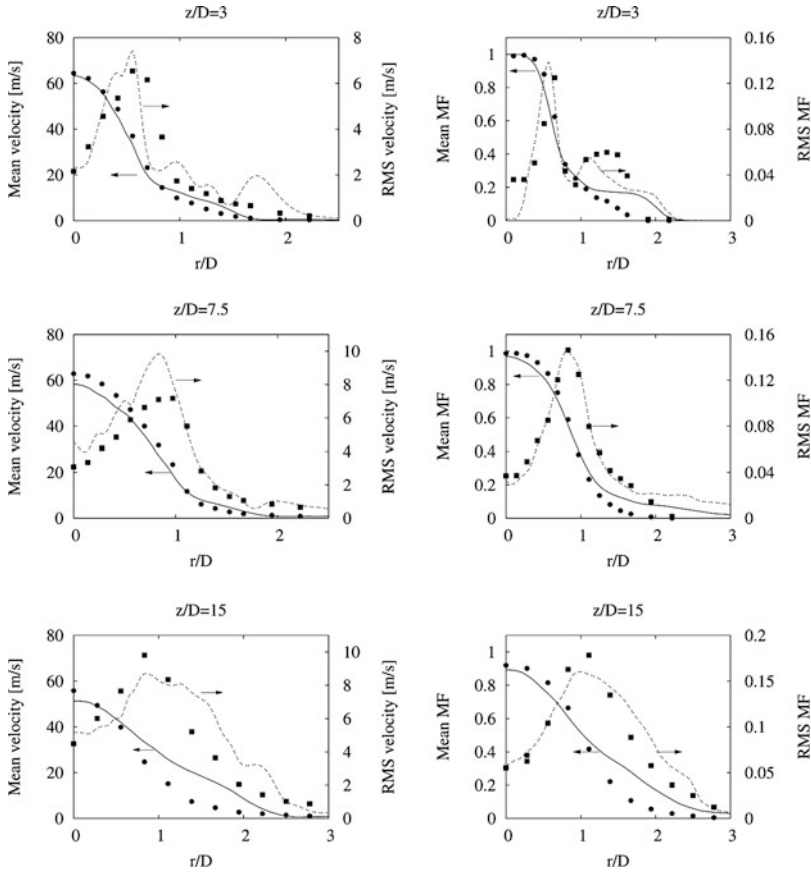
Fig. 3 Radial profiles of mean and RMS axial velocity and mixture fraction at three downstream locations for Flame D. *Symbols* denote experimental values [3,4], while the *solid* and *dashed lines* present the mean and RMS values of LES-CMC (reference case of Table 2)

Table 2 Summary of different parameters in combustion model study. The meaning of each numerical method can be found in Table 1

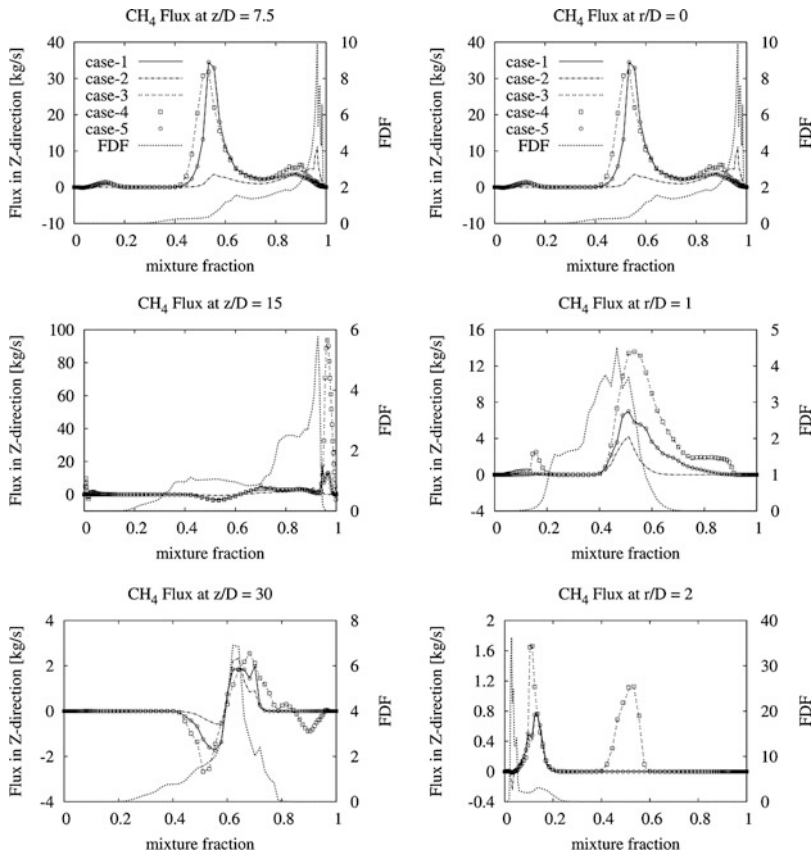| Name	Combustion model	Flow and mixing field	CMC grid resolution
case-1 (reference case)	CMC-1, flux-1, $D_{\eta,2}$		
case-2	CMC-2, flux-1, $D_{\eta,2}$	variance-2	
case-3	CMC-1, flux-2, $D_{\eta,2}$	Sc_2, $Sc_{t,1}$	
case-4	CMC-1, flux-2, $D_{\eta,1}$	$C_{\xi,1}$	$8 \times 8 \times 80$
case-5	CMC-1, flux-1, $D_{\eta,3}$		

Fig. 4 Axial (*left*) distribution along the centerline and radial (*right*) distribution at $z/D = 7.5$ of convective fluxes in z-direction of CH_4 for a time step (Sandia Flame D)

The investigations of fluxes in other species show that fluxes in different species follow the same tendency of CH4 fluxes in Fig. 4. It can be observed that case-2, case-3 and case-4 produce different convective fluxes compared with the reference case (case-1). However, case-3 and case-4 produce similar flux, which means their conditional scalar predictions should not be different. Therefore, case-3 is chosen for the further parametric studies. Fluxes of case-1 and case-5 are similar and also case-3 and case-4 are similar because of low effects of different D_η models on the convective term. Since case-1, case-2 and case-3 produce different convective fluxes, the conditional scalar predictions from these cases should differ from each other.

In next step, the statistical results of three cases (case-1, case-2 and case-3) are sampled over 30,000 time steps for the statistics to investigate the different effects of combustion model parameters and to validate with the experiment.
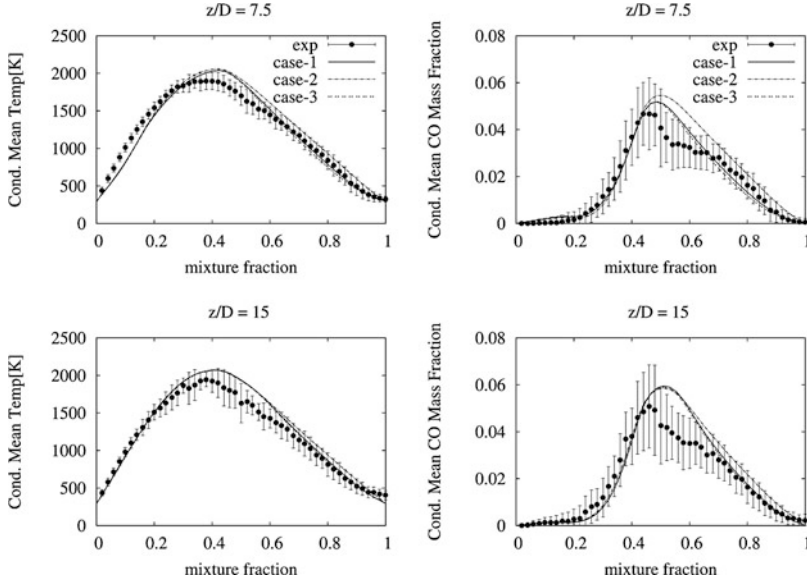
Fig. 5 Conditional profiles of cross-sectionally averaged temperature and CO at two different downstream positions in mixture fraction space for Flame D. *Symbols* are experimental data [4], while the *solid*, *dashed* and *dotted lines* present the results of LES-CMC in different cases in combustion model (Table 2)

Conditionally Filtered Reactive Scalars

As in CMC methodology, species mass fraction are analyzed in mixture fraction space, the efficiency of the combustion model can be decoupled from flowfield predictions. Therefore, the performance of each case of combustion model can be directly considered from conditional profiles. Initial values for the conditional reactive species are obtained from the SLFM solution.

A good agreement of case studies with experiments is shown in Figs. 5 and 6. The conditional mean temperature and the conditional mean mass fraction of CO, CH_4 and H_2 are given in both figures as a representative of intermediate products, fuel and radicals. Note that the error bars indicate the conditional RMS and they are only plotted to illustrate the turbulent level of each scalar. The reason of different predictions between case-1 and case-2 on the rich side ($\eta > 0.35$) belongs to two different sets of convective fluxes which are calculated from two CMC formulations. Because of the lack of FDF-weighting function in convective term, the low convective fluxes on the rich side are generated in the upstream positions of case-2. These can be observed in Fig. 7. Therefore, case-2 (non-conservative CMC) usually overpredicts on the rich side of mixture fraction in temperature, radical and intermediate product, while the underpredictions occur in the fuel.
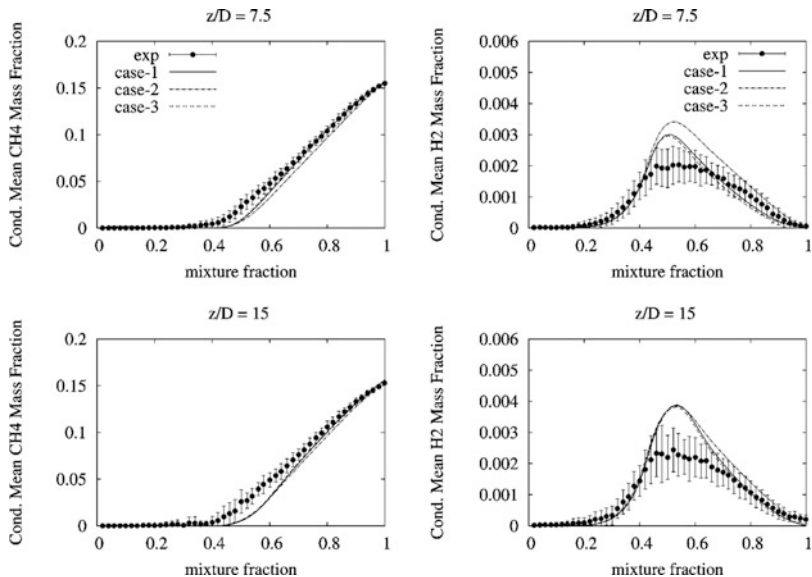
Fig. 6 Conditional profiles of cross-sectionally averaged CH_4 and H_2 at two different downstream positions in mixture fraction space for Flame D. *Symbols* are experimental data [4], while the *solid*, *dashed* and *dotted lines* present the results of LES-CMC in different cases in combustion model (Table 2)
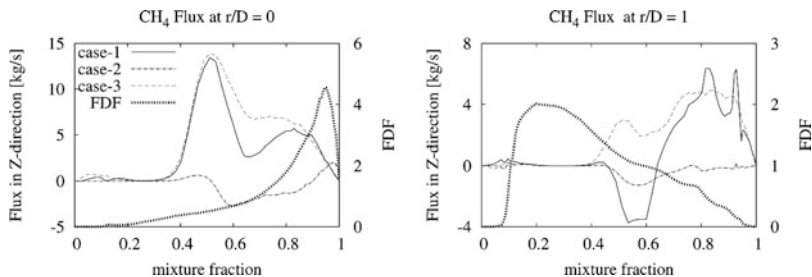

Fig. 7 Radial distribution of mean convective fluxes in z-direction of CH_4 at $z/D = 7.5$ (Sandia Flame D). The *solid*, *dashed* and *dotted lines* present the results of LES-CMC in different cases and FDF (reference case) in combustion model (Table 2)

It can be observed from the Figs. 5 and 6 that case-1 (conservative CMC) shows more accurate results than case-2. Cross-sectional simulation results from case-3 hardly differ from case-1, even though the convective fluxes from both cases are different (Fig. 7). The reason can be explained by using FDF value for each CMC cell in the same cross section to calculate the cross-sectional averages. If the conditional predictions between two cases of any CMC cell have a difference where the low FDF is calculated in mixture fraction space, the conditional predictions in cross-sectional averages will be similar.

Table 3 Summary of different cases in CMC grid resolution study

Name	CMC grid resolution	Flow and mixing fields	Combustion model
res-1	$4 \times 4 \times 80$	variance-2	
res-2	$8 \times 8 \times 80$	$Sc_2, Sc_{t,1}$	CMC-1, flux-1
(reference case)			$D_{\eta,2}$
res-3	$16 \times 16 \times 80$	$C_{\xi,1}$	

2.3.3 Parametric Study of CMC Grid Resolution

As described in Table 1, three cases of CMC grid resolution are varied, while the same conditions of flow and mixing field (variance-2, Sc_2, $Sc_{t,1}$ and $C_{\xi,1}$) and CMC combustion model (CMC-1, flux-1 and $D_{\eta,2}$) are set up. The variations of the CMC cells in each $x-$ and $y-$ direction are 4 cells for case-1, 8 cells for case-2 (reference case) and 16 cells for case-3 with the same 80 CMC cells in $z-$ direction, as summarized in Table 3.

Since the CMC resolution varies in the radial distribution for three case studies, the radial distribution of conditional value should show more prominent features. Therefore, the radial distribution of mean scalar are investigated at position $z/D = 3$, 7.5 and 15. The mean temperature and CO predictions in radial distributions are shown in Fig. 8.

It can be seen from position $z/D = 3$ that res-2 and res-3 perform better than res-1 since there is an underprediction of the temperature for res-1 in this position. Predictions of res-3 can capture the highest value of CO at position $z/D = 7.5$. Moreover, predictions from res-3 ($16 \times 16 \times 80$ for CMC cells) match better with the experiments than the others at position $z/D = 15$ which show a great advantage of small CMC cells in this resolution. A reason may relate to the size of CMC cell which the big size of CMC cell may predict inaccurately in which a high level of mixture fraction gradient occurs. However, an increasing CMC resolution from res-2 to res-3 requires more computational time than 60 %. Considering the computational time and results from all CMC resolutions, the appropriate resolution is res-2 ($8 \times 8 \times 80$ for CMC cells) for Flame D.

2.4 Summary

In this section, parametric studies of LES-CMC are carried out for the Sandia Flame D. The parameter studies comprised investigations of flow and mixing field, variants of the CMC combustion model parameters and CMC grid resolution.

Flame D is used to investigate the influences of various flow and mixing field parameters on the simulation results. These parameters, which are $Sc = 0.7$, $Sc_t = 0.4$ and $C_\xi = 0.2$, are optimal values and thus, they are used for further
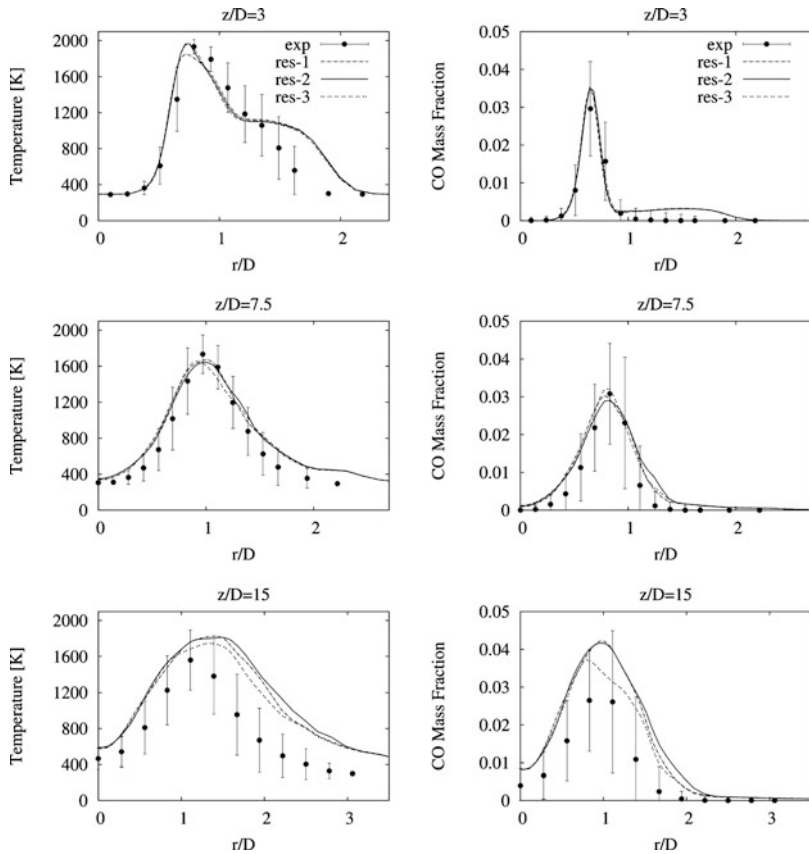
Fig. 8 Radial profiles of mean temperature and CO for Flame D. *Symbols* are experimental data [4], while the *solid*, *dashed* and *dotted lines* present the results of LES-CMC from the different CMC grid resolutions (Table 3)

studies of Flame D, as well as for Flames E and F. Values of velocity variance of inflow generator, however, depend on the physical inflow of each flame. It should be noted that an adjustment of the velocity variances is carried out to reduce the high level of turbulence which may come from the implementation of inflow generator. Suitable inflow variances for Flame D are found to be $\frac{2}{3}$ of the measured variances at $z/D = 0.14$ of these flames, respectively.

Parameter studies of different variants of the CMC combustion model are carried out to find the most suitable model. Initial studies of the CMC fluxes have shown that the effect of turbulent diffusivity modelling is negligible. However, a comparison of CMC models, which varies the CMC formulation (conservative vs. non-conservative), reveals considerable differences. Moreover, some slight differences between two methods of CMC convective flux approximation (cell face vs. cell centre based) are detected. Therefore, three dominant cases which differ in both

Table 4 Test cases for the LES-CMC model

	Test cases		
	LES cells	CMC cells	Flux implementation
Bluff-body flame, HM1	$218 \times 218 \times 320$	$16 \times 16 \times 80$ $24 \times 24 \times 80$	Various
4 lifted flames	$96 \times 96 \times 480$	$16 \times 16 \times 80$ $16 \times 16 \times 160$	Various

numerical aspects are investigated for further studies. Conditional mean scalars, which are averaged in the same cross section, show that the conservative CMC formulation with computing convective fluxes based on LES cells located at the CMC cell faces (case-1) is similar to the one with computing convective fluxes based on CMC cell centers (case-3). This can be explained by the low FDF values where the differences of predictions occur in a CMC cell. Consequently, the conditionally averaged predictions with FDF weighting create the similar results over a cross section. Generally, conditional predictions reveal that case-1 can capture better mean measurements than case-2 (the non-conservative formulation using the same flux approximation). This is because the variation of FDF-weighted convective fluxes in different directions of case-1 allows the predictions to be more accurate.

Three different CMC grid resolutions ($4 \times 4 \times 80$, $8 \times 8 \times 80$ and $16 \times 16 \times 80$) are examined in order to find the appropriate number of CMC cells for Sandia Flame D. Basically, the best predictions are found in CMC grid resolution of $16 \times 16 \times 80$. However, the reasonable resolution for Flame D is $8 \times 8 \times 80$ CMC cell due to the computational cost with efficient performance.

3 Future Study Cases

In order to show advantages of conservative CMC, more complicated flames are required for the simulations. Therefore, future test cases will be the Sydney bluff-body flame, HM1, with $218 \times 218 \times 300$ cells for LES for two CMC mesh sensitivity studies. Moreover, four lifted flames investigated at Berkeley [5, 6] and Calgary [7] will be examined (two Berkeley flames and two Calgary flames). The summation of all test cases can be found in Table 4.

4 The Usage of Computational Resources

The fine grid simulation results, which are presented here, have been performed on NEC Nehalem Cluster with 80 processors due to scalability tests for LES-CMC. The using of parallel program MPI and vectorization compiler let the code runs

faster. An approximate wall time is around 48 h per summited job. The analysis of all parametric studies from Table 1, of Flames D, E and F corresponds to 450,000 CPU hours. The amount of CPU use for Sandia Flame series is appropriate to the requirements of computational resources, 450,000 CPU hours for all test cases in future.

References

1. S. Navarro-Martinez, A. Kronenburg and F. Di Mare. Conditional moment closure for large eddy simulations. *Flow, Turb. Combust.*, 75:245–274, 2005.
2. S. Navarro-Martinez and A. Kronenburg. LES-CMC simulations of a turbulent bluff-body flame. *Proc. Combust. Inst.*, 31:1721–1728, 2007.
3. Ch. Schneider, A. Dreizler, J. Janicka and E.P. Hassel. Flow field measurements of stable and locally extinguishing hydrocarbon-fulled jet flames. *Combust. Flame*, 135:185–190, 2003.
4. R.S. Barlow and J. Frank. Piloted CH_4/Air Flames C,D,E, and F - Release 2.1. *CA*, 94551–0969, 2007.
5. R. Cabra, T. Myrvold, J.-Y. Chen, R. W. Dibble, A. N. Karpetis, and R. S. Barlow Simultaneous laser Raman-Rayleigh-LIF measurements and numerical modeling results of a lifted turbulent H2/H2 jet flame in a vitiated co-flow. *Proc. Combust. Inst.*, 29:1881–1888, 2002.
6. R. Cabra, J.-Y. Chen, R. W. Dibble, A. N. Karpetis, and R. S. Barlow. Lifted methane-air jet flames in vitiated co-flow. *Combust. Flame*, 143:491–506, 2005.
7. T. Leung and I. Wierzba The effect of co-flow stream velocity on turbulent non-premixed jet flame stability. *Proc. Comb. Inst.*, 32(2):1671–1678, 2009.